J. Med. Chem. **1998,** *41,* 798−807

Dihydropyrancarboxamides Related to Zanamivir: A New Series of Inhibitors of Influenza Virus Sialidases. 2. Crystallographic and Molecular Modeling Study of Complexes of 4-Amino-4*H*-pyran-6-carboxamides and Sialidase from Influenza Virus Types A and B

Neil R. Taylor,*[,†,⊥] Anne Cleasby,[†] Onkar Singh,[†] Tadeusz Skarzynski,[†] Alan J. Wonacott,[†] Paul W. Smith,[‡] Steven L. Sollis,[‡] Peter D. Howes,[‡] Peter C. Cherry,[‡] Richard Bethell,[§] Peter Colman,[∥] and Jose Varghese*[,∥]

Departments of Biomolecular Structure, Enzyme Medicinal Chemistry, and Enzyme Pharmacology, Glaxo Wellcome Research and Development Limited, Medicines Research Centre, Gunnels Wood Road, Hertfordshire, SG1 2NY, U.K., and Biomolecular Research Institute, Parkville, 3052 Victoria, Australia

Received June 6, 1997

The first paper in this series (see previous article) described structure−activity studies of carboxamide analogues of zanamivir binding to influenza virus sialidase types A and B and showed that inhibitory activity of these compounds was much greater against influenza A enzyme. To understand the large differences in affinities, a number of protein−ligand complexes have been investigated using crystallography and molecular dynamics. The crystallographic studies show that the binding of ligands containing tertiary amide groups is accompanied by the formation of an intramolecular planar salt bridge between two amino acid residues in the active site of the enzyme. It is proposed that the unexpected strong binding of these inhibitors is a result of the burial of hydrophobic surface area and salt-bridge formation in an environment of low dielectric. In sialidase from type A virus, binding of the carboxamide moeity and salt-bridge formation have only a minor effect on the positions of the surrounding residues, whereas in type B enzyme, significant distortion of the protein is observed. The results suggest that the decreased affinity in enzyme from influenza B is directly correlated with the small changes that occur in the amino acid residue interactions accompanying ligand binding. Molecular dynamics calculations have shown that the tendency for salt-bridge formation is greater in influenza A sialidase than influenza B sialidase and that this tendency is a useful descriptor for the prediction of inhibitor potency.

Introduction

Zanamivir (**1**, also known as 4-guanidino-Neu5Ac2en and GG167) (Chart 1) was the first potent inhibitor of influenza virus sialidase (also known as neuraminidase, NA) to be discovered.[1] The compound has been shown to inhibit viral replication in vitro,[1] in vivo (mouse and ferret models),[1] and in experimental infections in human volunteers.[2] The search for new compounds active against the enzyme has resulted in the discovery of inhibitors related to zanamivir which contain amide groups in place of the glycerol substituent. In the previous paper in this series we described the initial discovery and structure−activity relationships (SAR) of these carboxamides. Herein we report the protein crystallography and molecular modeling experiments that have been carried out on representative carboxamide analogues in order to provide detailed information on the binding mode of these types of inhibitors and to identify the basis of the selectivity between enzyme from influenza virus types A and B. A preliminary account of this work has been described elsewhere.[3]

Chart 1

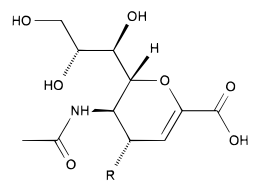

1 R = 

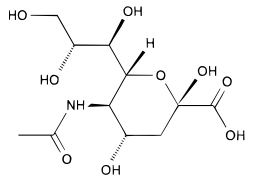

2

3 R = OH
4 R = NH_2

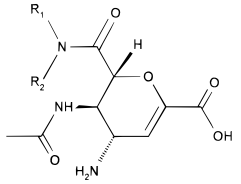

5a R_1 = $PhCH_2CH_2$ R_2 = H
b R_1 = $PhCH_2CH_2$ R_2 = Me
c R_1 = $PhCH_2CH_2$ R_2 = Et
d R_1 = $PhCH_2CH_2$ R_2 = Propyl
e R_1 = $PhCH_2CH_2$ R_2 = CH_2CHMe_2

Nine subtypes of sialidase have been identified for type A influenza, N1 to N9, while no subtypes have been isolated for type B virus. The first crystallographic

* Author to whom correspondence should be addressed.
† Department of Biomolecular Structure.
‡ Department of Enzyme Medicinal Chemistry.
§ Department of Enzyme Pharmacology.
∥ Biomolecular Research Institute.
⊥ Present address: BASF Bioresearch Corp., 100 Research Dr., Worcester, MA 01605-4314.

S0022-2623(97)00375-0 CCC: $15.00 © 1998 American Chemical Society
Published on Web 02/18/1998

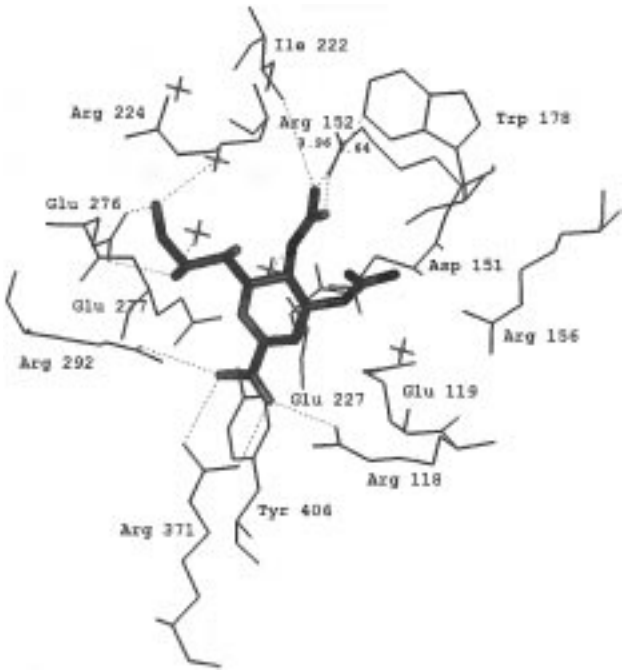

Figure 1. Active site of the complex of zanamivir, **1**, and influenza B sialidase showing the major protein−ligand hydrogen-bonding and van der Waals interactions.

Table 1. IC_{50} Values for C4-Modified Neu5Ac2En Inhibitors

	IC_{50} (μM)	
compd	A sialidase	B sialidase
1	0.005	0.004
2	∼1000	∼1000
3	8.6	15
4	0.32	0.41

study on the enzyme was performed with subtype N2, from virus A/Tokyo/3/67 and RI/5-/57,[4−6] and this structure and its complex with sialic acid were used in the design of zanamivir.[1] Subsequently, the structures of sialidase from three other strains of influenza virus have been characterized, namely, from A/Tern/Australia/G70c/75, subtype N9,[7] from B/Beijing/1/87,[8] and from B/Lee/40.[9] Although the sequence homology between sialidase from type A and B virus is not high (typically around 30%), the conserved residues of the active sites from all influenza sialidases superimpose very closely with both the main-chain and side-chain atom positions showing a close correspondence. The structural similarities between the active sites of influenza A and B sialidases are reflected in the SAR for the sialic acid (also known as Neu5Ac and NANA, **2**)-based inhibitors listed in Table 1.

Active-Site Architecture and Ligand Interactions. The crystal structures have previously been determined for complexes of sialidase with inhibitors **1**[10]and **2**[11] for A virus and **2**[8]and **3**[12] for B virus. In our studies the structures of the complex with **4** have also been solved (unpublished results). In all cases the ligand binds in a closely similar manner. The common pattern of protein−ligand interactions is illustrated by the complex of sialidase from influenza virus B/Beijing and zanamivir, **1**, shown in Figure 1. (The amino acid numbering scheme for sialidase from both types A and B virus employed throughout this report corresponds to the numbering scheme used for N2 enzyme from A/Tokyo/3/67.) The key protein−ligand interactions which are common to all complexes are highlighted in the diagram. These interactions consist of strong charge−charge- and charge−partial charge-based hydrogen bonds and some highly specific hydrophobic contacts. The carboxylic acid of the ligand makes charge−charge-based hydrogen bonds to a cluster of three arginine residues, 118, 292, and 371, including a planar salt bridge to 371. The acetamido fragment forms hydrogen bonds to Arg 152 and a buried water molecule, while the methyl group makes favorable hydrophobic contact with two residues, Trp 178 and Ile 222. A bidentate interaction occurs between the two terminal hydroxyl groups of the glycerol moiety and residue Glu 276. The sugar ring atom of **1** does not appear to make strong interactions to any active-site residues, although there may be a weak electrostatic interaction between the ring oxygen and Arg 292.

The guanidino group of **1** occupies a small pocket on the side of the binding cavity. It is involved in three charge−charge-based interactions, with amino acid residues Glu 119, Asp 151, and Glu 227. In addition, the basic substituent forms a geometrically favorable bidentate interaction to the backbone carbonyl group of Trp 178, through its terminal NH_2 groups, and a hydrogen bond to a bridging water molecule. This set of hydrogen bonds may reinforce other protein−ligand and protein residue−residue interactions in a cooperative fashion, resulting in a strong network of hydrogen-bonding interactions. In uncomplexed sialidase, and also in the complexes with **2**−**4**, a water molecule occupies the pocket on the side of the binding cavity formed by the three charged residues. Upon binding of zanamivir, this water molecule is displaced by the guanidino substituent, and this may contribute a favorable entropic factor to the binding. The dramatic improvement in binding affinity of **1** relative to the 4-hydroxy analogue **3** (approximately 3 orders of magnitude) is believed to be the result of (i) electrostatic forces, (ii) hydrogen-bonding network, and (iii) entropic contribution.

The superimposition of sialidase complexes containing zanamivir, **1**, and Neu5Ac2en, **3** (in either influenza A or B enzyme), demonstrates that replacement of the hydroxyl substituent by the guanidinium group only slightly alters the positions of adjacent protein side chains Arg 156, Asp 151, Glu 119, and Glu 227 and does not affect any distal residues. Figure 2 illustrates the overlap for influenza B (complex with **3** solved by Burmeister et al.[12]). Residue Arg 156 appears to be repelled slightly from the guanidino substituent, residue Asp 151 adjusts conformation to form hydrogen bonds to the basic group, and the two acids Glu 119 and Glu 227 are in slightly different conformations. The fact that the conformations of active-site residues are not significantly changed by the guanidino group is another important aspect of the tight binding of zanamivir.

Our previous experience with SAR studies involving sialidase has shown that the structural differences between the active sites of influenza A and B enzyme do not significantly affect binding affinity. Furthermore, high inhibitory activity was achieved without major conformational changes occurring in the active-site residues (consistent with current paradigms in

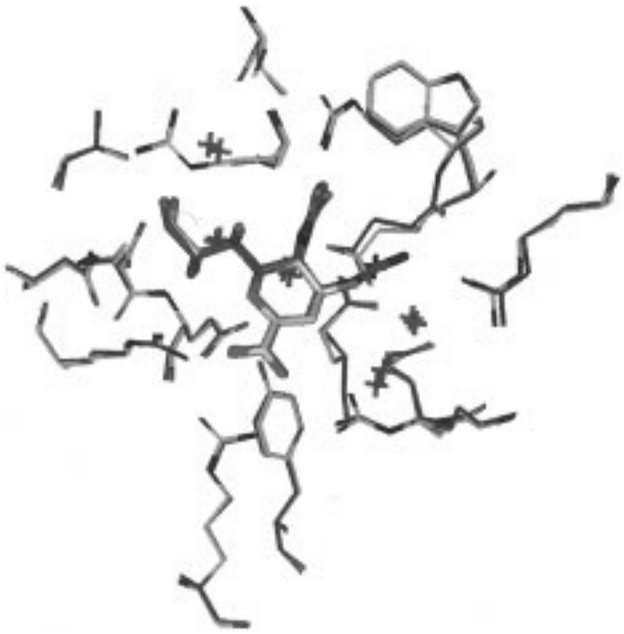

Figure 2. Superimposition of the active sites of the influenza B sialidase complexes containing zanamivir, **1** (carbon atoms colored green), and Neu5Ac2en, **3** (carbon atoms colored orange). The two structures can be seen to superimpose very closely, with only minor differences in the vicinity of the C4 substituent. The water molecule that is displaced from the C4 pocket by the guanidinium (highlighted in black) superimposes on the "lower" NH_2 group.

Table 2. IC_{50} Values for Carboxamide-Containing Analogues of Zanamivir

			IC_{50} (μM)	
compd	R_1	R_2	A sialidase	B sialidase
5a	$PhCH_2CH_2$	H	12	67
5b	$PhCH_2CH_2$	methyl	0.32	51
5c	$PhCH_2CH_2$	ethyl	0.005	8.2
5d	$PhCH_2CH_2$	propyl	0.002	3.6
5e	$PhCH_2CH_2$	CH_2CHMe_2	0.014	110

protein structure-based drug design). In this report we describe a very different scenario, one in which subtle structural differences appear to have dramatic impact upon ligand affinities and where potent activity is associated with significant changes in active-site amino acid conformation. The differences between the active sites of influenza A and B sialidase are thus highly relevant to the selectivity of the carboxamide-containing inhibitors, as elucidated below. (IC_{50} values are listed in Table 2.)

Structural Comparisons of Flu A and Flu B Sialidase. Despite the many structural similarities in the active sites of sialidase from influenza A and B, close inspection of the crystal structures shows that there are some interesting differences,[10] particularly at position 405 and in the vicinity of residue Arg 224. Residue 405 in enzyme from influenza B is a tryptophan (the largest natural amino acid), whereas in enzyme from influenza A, the residue is a glycine (the smallest natural amino acid). In influenza A sialidase, water molecules and the Cδ atom of Ile 427 occupy the region of space that the aromatic group occupies in influenza B sialidase, between arginine residues 118 and 371. Figure 3a,b illustrates this region of the active sites in sialidase from influenza A and B. The floor of the active site of influenza B sialidase is sterically more crowded than in influenza A sialidase, indicating that residues in influenza B sialidase might be tightly constrained to the observed positions in the uncomplexed enzyme. Interestingly, the active-site residues of influenza A and B sialidase in the vicinity of residue 405, such as Arg 118, Arg 371, and Tyr 406, superimpose very closely.

Around the conserved amino acid Arg 224 there are a number of differences between the two active sites (see Figure 3c–f). First, and most significantly, in influenza B sialidase there is a hydrogen bond between Arg 224 and the serine at position 250. In influenza A sialidase, no such hydrogen bond exists since residue 250 is an alanine. These structural features are shown in Figure 3c,d. Second, despite the fact that in the two enzymes the acidic oxygen atoms of Glu 276 occupy very similar relative positions, the side-chain conformations are different (influenza A sialidase, $\chi^1 = -69$, $\chi^2 = -169$; influenza B sialidase, $\chi^1 = 67$, $\chi^2 = 175$). This difference appears to arise as a consequence of an unconserved residue deeper into the core of the protein, at position 240. In the enzyme from influenza A, there is a valine at position 240, while in enzyme from influenza B, the residue is a methionine (see Figure 3e,f). In influenza A sialidase, the small amino acid provides space for two water molecules which hydrogen bond to the hydroxyl of Thr 242, the backbone oxygen atom of Val 240, and a third (conserved) water molecule. In the enzyme from influenza B, the terminal methyl group of the Met residue makes hydrophobic contact with the methyl of Thr 242 and the Cα of Glu 276. These differences are highlighted in Figure 3e,f. It appears that the different side-chain conformations of the acid residue are a result of the different environments around the Cα atom—there is a hydrophilic environment around the side chain of Glu 276 in influenza A sialidase, whereas there is a hydrophobic environment around the side chain in influenza B sialidase.

Results and Discussion

Crystal Structure of Influenza A Sialidase with 5-(Acetylamino)-4-amino-6-(phenethylpropylcarbamoyl)-5,6-dihydro-4*H*-pyran-2-carboxylic Acid (5d). The dihydropyran ring of **5d**, the carboxylic acid, and the acetamide group all bind to the A enzyme in approximately the same mode as observed for **1** and **2**.[10,11] Furthermore, the amino group occupies the pocket on the side of the binding cavity as in **4**, forming hydrogen bonds to Glu 119, Asp 151, and a water molecule. It is also involved in a favorable electrostatic interaction with Glu 227. However, significant differences from the complex containing **1**, and all previously described structures, are observed in the region where the carboxamide binds. Figure 4 illustrates the binding mode. The *N*-phenethyl-*N*-propylamide substituent fits into the "glycerol pocket" of the active site through a major rearrangement in the conformation of active-site residue Glu 276, a conformational change not previously observed. The side chain of this residue "folds down" and forms a new planar salt bridge with residue Arg 224 (hydrogen bond distances: Glu 276 Oϵ2···Arg 224 Nη1 = 2.8 Å and Glu 276 Oϵ1···Arg 224 Nϵ = 2.8 Å). A new hydrogen bond between Glu 276 and His 274 is also formed (Glu 276 Oϵ2···His 274 Nϵ2 = 2.8 Å), as is a new

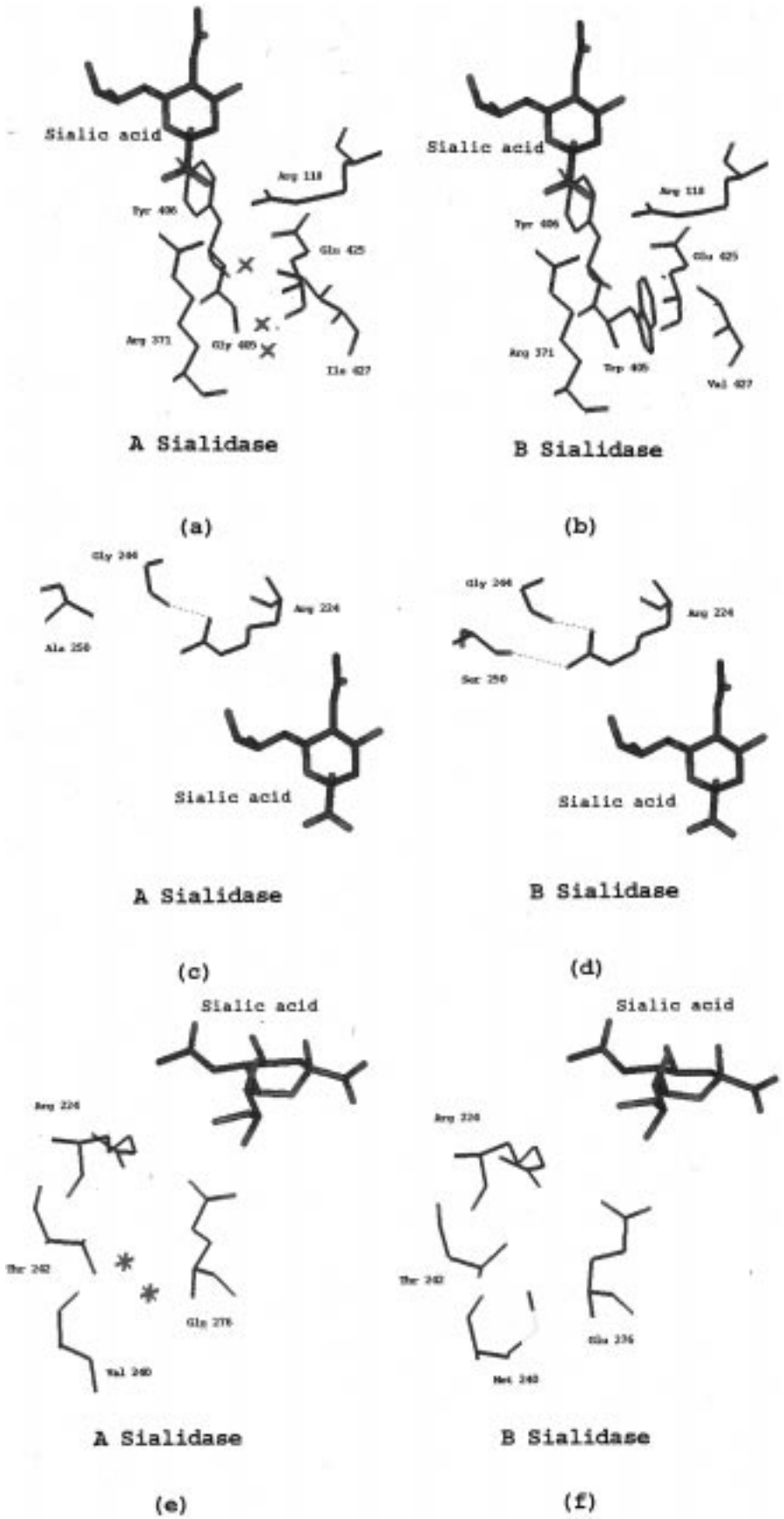

Figure 3. Comparison of the active sites of influenza A (A/Tern/N9) and influenza B (B/Beijing) sialidase: (a,b) top views of A and B sialidase in the vicinity of residue 405, in influenza A residue 405 is a glycine, whereas in influenza B it is a tryptophan; (c) top view of A sialidase in the vicinity of residue 224 showing residue Arg 224 hydrogen-bonded to Gly 224; (d) top view of B sialidase in the vicinity of residue 224 showing Arg 224 hydrogen-bonded to both Gly 224 and Ser 250; (e) side view of A sialidase showing that the protein environment around the Glu 276 main-chain atom is hydrophilic (the oxygen atoms of water molecules are displayed as red stars); (f) side view of B sialidase showing that the protein environment around the Glu 276 main-chain atom is hydrophobic. The different environments around Glu 276 may account for the difference in the side-chain torsion angles (see text).

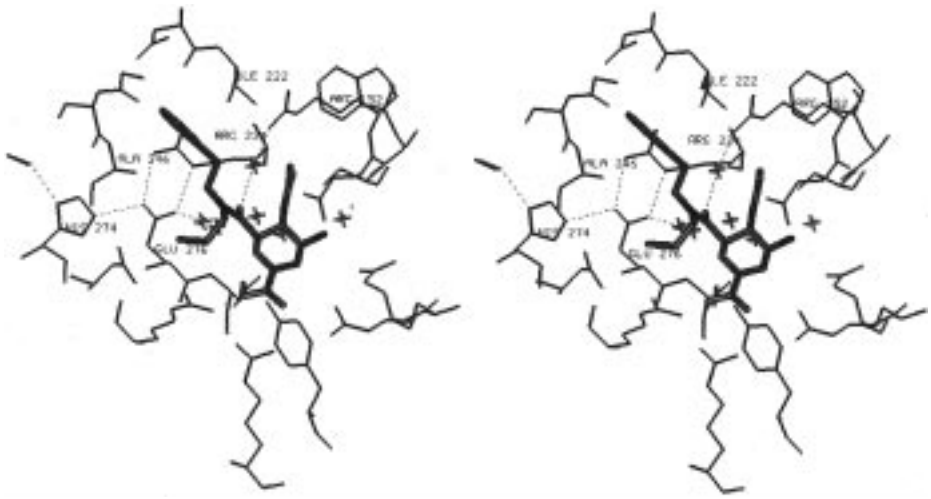

Figure 4. Stereoview showing the binding of **5d** to influenza A sialidase. The phenethyl group of the tertiary amide fits into the trans-pocket, between residues Ile 222 and Ala 246, and the propyl group occupies the cis-pocket, created by the conformational change in residue Glu 276. The planar salt-bridging interaction between Glu 276 and Arg 224 is illustrated by broken lines, as are other associated hydrogen bonds.

hydrogen bond with a buried water molecule (Glu 276 Oϵ1···Wat O = 2.9 Å). The salt-bridging conformation of Glu 276 thus enables all four of the lone pairs on the acidic oxygen atoms to be involved in favorable hydrogen-bonding interactions with neighboring protein groups. Finally, a water-mediated hydrogen-bonding interaction is observed between the carbonyl oxygen atom of the tertiary amide and Arg 152. This interaction is illustrated in Figure 4.

The propyl moiety of the tertiary amide substituent occupies a region in the active site created by the rearrangement of Glu 276. This new region is partially lipophilic in nature and is herein referred to as the cis-pocket. All of the amino acid residues which define the cavity, Ala 246, Asn 249, Glu 276, Glu 277, and Arg 292, make close van der Waals contacts between at least one of their carbon atoms and the terminal ethyl moiety of the ligand. The phenethyl group occupies a narrow channel between two lipophilic residues, Ile 222 and Ala 246, with residue Arg 224 defining the channel floor. This cleft is referred to here as the trans-pocket. Our cis and trans notation reflects the configuration about the amide bond in the ligand.

Although the side chain of Glu 276 adopts a completely new conformation in the complex with **5d**, there is minimal disruption in the surrounding protein structure. The positions of Arg in the salt bridge, of residue His 274, and of the main-chain atoms of residues 276−275 are all very similar to the positions in the uncomplexed enzyme. A buried water molecule, which in unliganded protein bridged between adjacent buried water molecules and one of the oxygen atoms of Glu 277, is pushed deeper into the base of the active site upon salt-bridge formation. This change in position of the water molecule (2.3 Å) displaces two neighboring buried water molecules (the change in positions are 0.6 and 0.2 Å) and creates a new hydrogen-bonded network of water molecules between protein and ligand. The docking of the phenethyl group displaces two water molecules from the lipophilic cleft (water molecules that form a network from the carbonyl oxygen atom of Gly 244 to a terminal nitrogen atom of Arg 152). The protein loops which define the trans-pocket have similar positions in the complex with **5d** as in the complex with **1**. Tight binding of **5d** appears to be achieved (without the presence of the guanidino group) by (i) burial of hydrophobic surface area and release of water molecules from the active site of the protein and (ii) creation of new hydrogen-bonding interactions, including a planar salt bridge, in a region of low dielectric relative to that of bulk solvent.

Crystal Structure of Influenza B Sialidase with 5-(Acetylamino)-4-amino-6-(phenethylpropylcarbamoyl)-5,6-dihydro-4*H*-pyran-2-carboxylic Acid (5d). The ligand binds to the active site of influenza B sialidase in roughly the same mode as seen for influenza A sialidase, with a planar salt bridge between Glu 276 and Arg 224 being formed (hydrogen bond distances: Glu 276 Oϵ2···Arg 224 Nη1 = 2.8 Å and Glu 276 Oϵ1··· Arg 224 Nϵ = 2.8 Å), a new hydrogen bond between Glu 276 and a buried water molecule (distance: Glu 276 Oϵ1···Wat O = 2.7 Å), the propyl group occupying the newly created cis-pocket, and the phenethyl group fitting into the lipophilic trans-pocket. However, the crystal structure reveals that the active site of influenza B sialidase does not accommodate the carboxamide moiety as well as the active site of influenza A sialidase. Figure 5 illustrates the refined structure of **5d** bound in the influenza B enzyme (atoms colored by type) and superimposed onto the complex containing **1** (with atoms colored purple). Inspection of Figure 5 shows that most active-site residues superimpose closely except in the vicinity of the C6 substituent. In this region around the carboxamide group, the gylcerol pocket appears "pushed open" to fit the ligand and the new Glu 276-to-Arg 224 salt bridge. The major distortions occur in (i) the protein loop associated with Ala 246 which forms one side of the trans-pocket, (ii) the backbone atoms of Glu 276, (iii) the side chain of Arg 224, (iv) the side chain of His 274 which formerly was hydrogen-bonded to the loop associated with Ala 246, and (v) the side chain of residue Ser 250 which is no longer hydrogen-bonded to Arg 224 as a consequence of the new conformation of Glu 276. Analysis of the temperature factors in the complex reveals that many of the displaced protein groups have significantly higher values

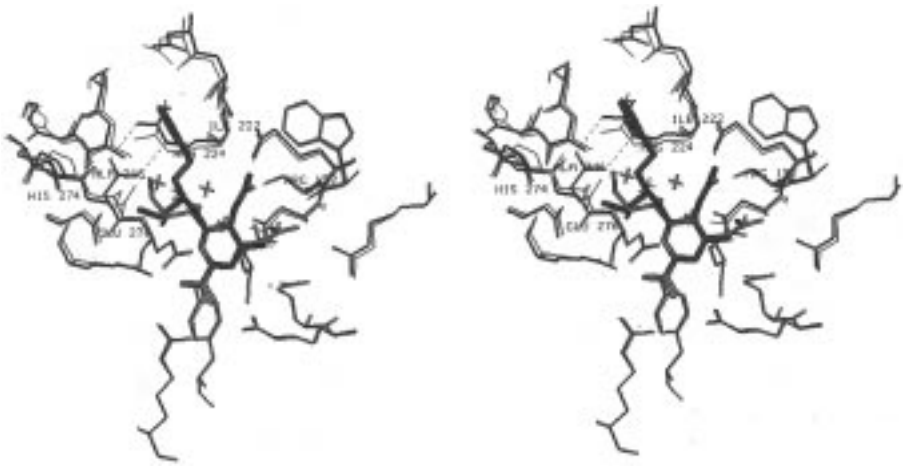

Figure 5. Stereoview of the superimposition of the active sites of the influenza B sialidase complexes containing **1** and **5d**. Overall, the active-site residues superimpose closely. The biggest difference between the two protein structures is in the neighborhood of the C6 substituent where ligand binding results in a small expansion of this region of the protein. In the complex with **5d**, distortions in the protein backbone occur at Glu 276, in the loops on both sides of the phenethyl moiety, and in the side chains of residues Ser 250 and Arg 224.

than in other complexes. This feature of the results is expanded in the following section. There are also changes in the hydrogen bond network associated with the buried water molecules bridging between protein and ligand. Docking of the carboxamide group causes one water molecule to be pushed deeper into the floor of the active site relative to its position in uncomplexed protein (change in position = 3.1 Å), and this, in turn, displaces two neighboring buried water molecules (displacements are 1.1 and 0.4 Å).

An interesting outcome of the crystallography is that the two independent monomers in the unit cell of the crystal have slightly different structures. In one monomer, the protein loop containing Ala 246 has lower temperature factors than in the other monomer (Figure 5 illustrates the monomer with the higher temperature factors). This discrepancy was traced to crystal packing forces: the monomer with the lower temperature factors makes contact with protein surface from another molecule in the crystal, thereby stabilizing the structure. In the same monomer there was evidence for two water molecules binding in the C4 pocket and interacting with the amino substituent. Previously, this pocket has only been observed to contain one water molecule. The position of the two waters shows a close similarity to the positions of the terminal nitrogen atoms of the guanidinium group in the complex with zanamivir, **1**. It appears that modifications at the C6 position result in subtle changes in the distal regions of the active site.

Comparison of Complexes with 5d in Influenza A and B. The structure−activity studies described in the previous article clearly demonstrate that inhibitors which contain tertiary amide groups are significantly more potent against influenza A sialidase than against influenza B sialidase. In like manner, the protein crystallography shows that the docking of the phenethylcarboxamide moiety is much less favored in influenza B sialidase than in influenza A sialidase. As described in the previous two sections, the binding of both the *cis*-propyl group and the *trans*-phenethyl group causes small but significant expansions in neighboring regions of the active site of influenza B sialidase, but not in the active site of sialidase from influenza A.

Figure 6 highlights what are believed to be the most significant differences between the binding of the carboxamide group to sialidase from influenza A and B. Figure 6a,b shows that the side-chain conformations of Glu 276 are different in the complex with **1** (although there is a close relationship in the relative positions of the acidic oxygen atoms) whereas the conformations are similar in complexation with **5d**. The diagrams show that in order for Glu 276 to form the salt bridge, B sialidase is required to undergo larger changes than A sialidase. We suggest that in influenza B sialidase there are energy penalties accompanying the rearrangement in the side-chain conformation of Glu 276 that do not occur in A sialidase. We mentioned previously that the region adjacent to the main-chain atoms of Glu 276 is hydrophilic in influenza A sialidase whereas it is hydrophobic in influenza B sialidase (see Figure 3e,f). It is possible that this hydrophobic environment in B sialidase inhibits the side chain from changing conformation. In addition, extra energy penalties in influenza B sialidase may occur due to the higher steric crowding in the active site (as mentioned in the Introduction). Figure 6c,d shows some of the active-site residues color-coded according to temperature factor. It can be seen that binding of the bulky carboxamide group in B sialidase causes temperature factors in the protein to increase, whereas in A sialidase, the temperature factors remain unchanged. Also highlighted is a hydrogen bond between Glu 276 and His 274 which occurs in A sialidase but not in B sialidase. In the A enzyme, this interaction is part of a network of hydrogen bonds involving the Glu 276-to-Arg 224 salt bridge, a number of buried water molecules, and Gly 248, which is part of the loop that includes Ala 246. Interestingly, it is this loop which has very high temperature factors in B sialidase. Last, Figure 6d shows that a hydrogen bond between Ser 250 and Arg 224 which occurs in B sialidase complexed with **1** cannot form in the enzyme complex with **5d** due to the disorder in Ser 250 and the displacement of Arg 224. There is no corresponding change in hydrogen bonding in A sialidase (residue 250 is not conserved; see Figure 3c).

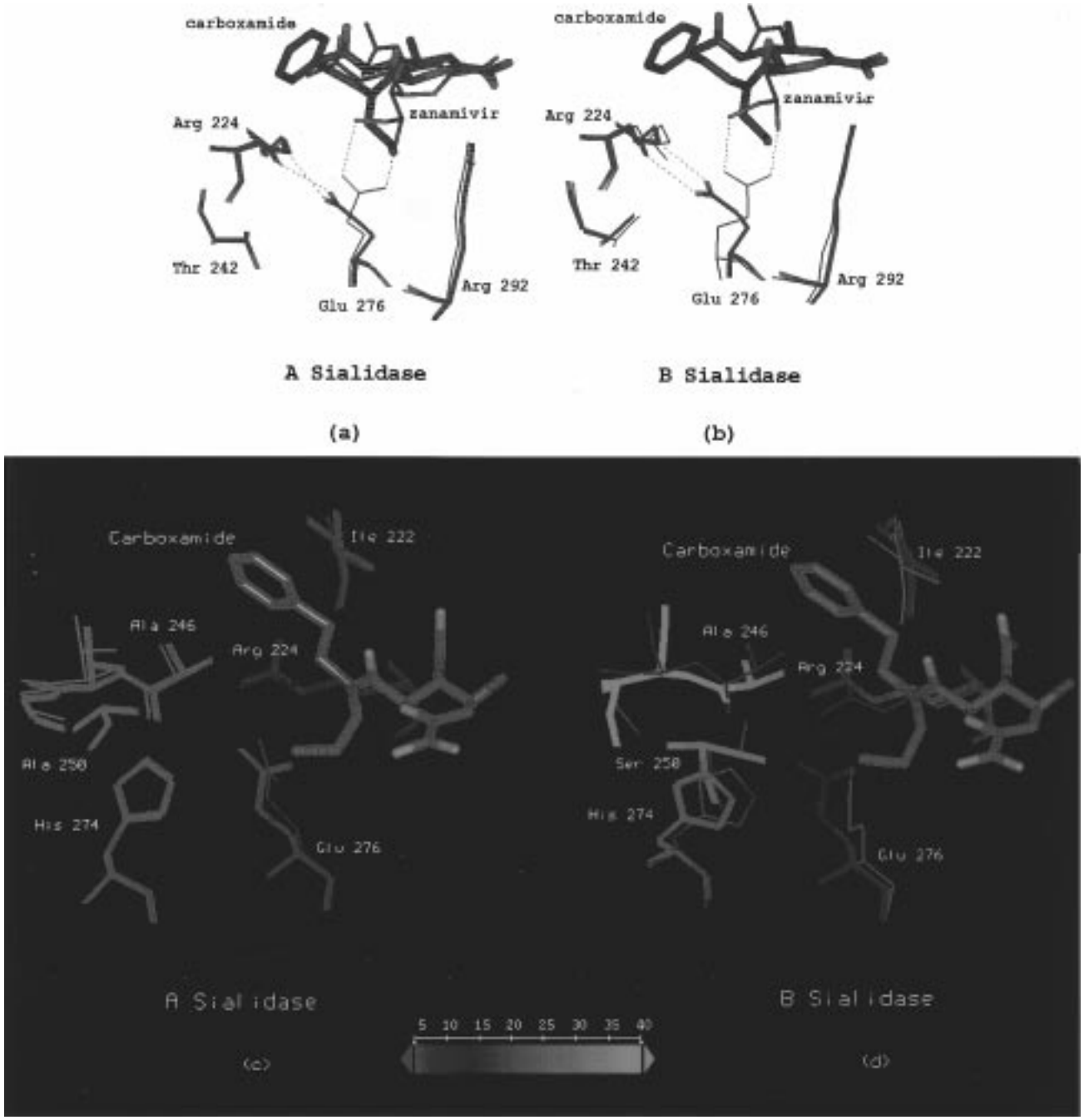

Figure 6. Comparison of the enzyme−inhibitor complexes of **1** (thin lines) and **5d** (thick lines) in influenza A and B sialidase: (a,b) rearrangement in Glu 276 from the bidentate interaction with the glycerol of zanamivir to the salt-bridging conformation with Arg 224 in the presence of carboxamide, the changes in both the side-chain and main-chain atoms of Glu 276 can be seen to be greater in B sialidase than in A sialidase; (c,d) changes in protein temperature factors and in hydrogen bonding induced by salt-bridge formation, temperature factors, which are color-coded according to the associated scale, can be seen to increase in B sialidase but not in A sialidase, and in A sialidase salt-bridge formation is accompanied by the creation of a new hydrogen bond to His 274, whereas in B sialidase it is accompanied by the loss of a hydrogen bond between Ser 250 and Arg 224.

Small conformational rearrangements of active-site amino acids on binding of inhibitors are commonly observed. However, as in the case of purine nucleoside phosphorylase[13] where active-site residues Asn 243 and Thr 242 are able to adopt one of two different hydrogen-bonding schemes, depending upon the nature of the bound ligand, crystallographic analyses were essential in order to understand and account for the SAR data.

Molecular Modeling. A molecular dynamics/energy minimization protocol was used to investigate the binding of the series of carboxamides **5a**−**e** to sialidase from influenza A and B. The protocol was designed specifically to (i) search conformational space of protein−ligand interactions in the vicinity of crystal structures, (ii) account for the structural effects of functional group substitution on ligand binding, and (iii) estimate the relative strengths of protein−ligand interactions.[14] The approach generates (i) a range of low-energy structures, which can be analyzed using interactive graphics, and (ii) sets of energy values, which can be compared with observed biological activities. The method has previously been shown to produce useful results in a study of the binding of C4-modified Neu5Ac inhibitors to influenza A sialidase.[15] Similar calculations were there-

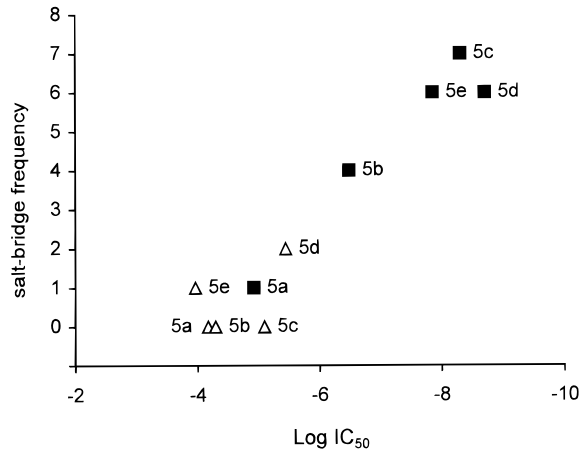

Figure 7. Trend between the experimental log IC_{50} values for compounds **5a**−**d** and the frequency of formation of the Glu 276-to-Arg 224 salt bridge within the set of 15 energy-minimized structures for each of the inhibitors. The squares correspond to influenza A sialidase and the triangles to influenza B sialidase.

fore done on the carboxamide-containing inhibitors to extend our understanding of both the structural and energetic aspects of binding to sialidase and also to look for correlations between the calculated results and the experimental affinities. Greater emphasis was placed on the analysis of the structural results than on the analysis of calculated energies because the interpretation of protein−ligand binding data only in terms of molecular mechanics-derived energies can be problematic (see, for instance, Williams et al.[16]).

The most striking aspect of the modeling results was the occurrence of planar salt bridges between Arg 224 and Glu 276 in the calculated low-energy structures, as observed in the crystal structures. The influence of bulky carboxamide groups on the conformation of Glu 276—its tendency to induce salt-bridge formation—was simulated in the dynamics calculations for both the influenza A and B sialidase complexes. Interestingly, the proportion of the low-energy structures that contained the salt bridge was much greater for influenza A sialidase than for influenza B sialidase and, furthermore, was generally the highest for inhibitors with the greatest activity. Figure 7 clearly illustrates the close correlation obtained between the experimental IC_{50} values and the number of calculated low-energy structures with the planar salt bridge. In this work, the criteria for salt bridging is defined to be a coplanar arrangement for the guanidinium and carboxy groups, with hydrogen-bonding distances of less than 3.3 Å. Although the trend between the IC_{50} values and the numbers of calculated planar salt bridges is good, we do not suggest that it applies for all inhibitors with lipophilic groups in place of the glycerol substituent. However, we did find it to be useful for estimating binding affinity in a number of instances.

Another interesting feature of the low-energy structures was the position of the *trans*-phenethyl group. In most of the calculated structures the aryl ring was located in the protein cleft, between residues Ile 222 and Ala 246. However, in some cases it had "popped out" of the cleft and into solution. This was more common for complexes involving influenza B than influenza A, and in both cases the frequency increased with increasing size of the cis-group. This observation is consistent with the crystallographic results, that the glycerol pocket in influenza B sialidase is unable to accommodate the bulky carboxamide group as well as influenza A sialidase.

In an attempt to explain these calculated results for influenza A and B sialidase, an analysis of the molecular mechanics energies was undertaken. In general, the calculated structures with the lowest energies correspond to structures containing the Glu 276-to-Arg 224 salt bridge. Furthermore, according to the molecular mechanics calculations, in influenza A sialidase there is a relatively large gain in binding enthalpy as the cis-group increases in size from the hydrogen atom to the propyl group, whereas in influenza B, the change is not significant. These results are a close reflection of the observed trends in experimental affinities. Examination of the separate contributions to nonbonding energy (van der Waals and Coulombic terms) demonstrated that salt-bridge formation is detrimental to the overall van der Waals interactions between amino acid residues. In other words, it appears that the conformational rearrangement in Glu 276 occurs with energy penalties associated with steric clashes. This is in agreement with the crystal structure data for uncomplexed sialidase; the hydrogen bonds that Glu 276 makes with solvent, coupled with favorable electrostatic interactions with both Arg 224 and Arg 292, appear to provide greater stability to the protein than does salt-bridge formation. Inspection of the calculated electrostatic energies revealed that ion-pair formation in a medium of relatively low dielectric (i.e., an environment shielded from solvent) does provide significant contribution to the binding enthalpy in the complexes with carboxamide groups.

An important component of the free energy of binding that molecular mechanics is unable to fully take into account involves the role of water molecules. We described above how some buried water molecules change position and create a new hydrogen bond network upon binding of the carboxamide group. Neither the angular dependence of the hydrogen bonds nor the cooperativity associated with the hydrogen bond network is modeled in the classical force field, and both of these factors may be significant. Entropy plays an important role in the binding; however, molecular mechanics does not take it into account. Although an entropy analysis of the binding of these ligands to sialidase was not undertaken, it is anticipated that $\Delta S_{solvent}$, the change in the entropy of water upon complex formation, would also favor the stability of the complexes ($\Delta S_{solvent}$ is significant when complexation is accompanied by the burial of large amounts of hydrophobic surface; see, for instance, Schulz and Schirmer[17]).

Conclusions

This paper describes the protein crystallography and molecular modeling experiments that have been done to characterize the binding mode of carboxamide analogues of zanamivir to influenza virus sialidase types A and B and to identify the basis of the selectivity between the two enzymes. The carboxamide-containing ligands were found to bind in the active sites of influenza A and B sialidase in the same mode, inducing

the formation of a previously unobserved planar salt bridge between amino acid residues Glu 276 and Arg 224. The strong binding of these inhibitors is believed to arise as a result of buried hydrophobic surface area and salt-bridge formation in an environment of low dielectric. Overall we found a number of subtle differences in the binding of **5d** to influenza A and B sialidase which help explain the differences in affinity. Analysis of the crystal structure data indicated that the bulky phenethylpropylcarboxamide group is not accommodated in the glycerol pocket in influenza B sialidase as well as in influenza A sialidase. In influenza B sialidase, binding of the carboxamide moiety causes a small expansion of the region of the protein around the pocket; distortions occur in the protein backbone at Glu 276 (adjacent to the propyl group), in the loop containing Ala 246 (which makes contact with the phenethyl group), and in Ser 250 and His 274 (residues which are adjacent to the salt bridge). Molecular modeling studies showed that in complexes of influenza A and B sialidase and carboxamide analogues of zanamivir, salt-bridge formation could be simulated in molecular dynamics calculations. It was found that salt-bridge formation was more frequently observed for inhibitors with the greatest activity. In contrast to previous SAR studies involving influenza virus sialidase, we have found that the small structural differences between the active sites of influenza A and B sialidase can have dramatic impact upon ligand affinities and that potent activity can be achieved with significant changes occurring in the conformations of active-site residues. Protein crystallography and molecular modeling have successfully combined to provide an explanation of the higher affinity of the carboxamide-containing inhibitors to influenza A sialidase, and this demonstrates the importance of these approaches to understanding protein−ligand interactions and to drug discovery.

Experimental Details

X-ray Crystallography. Sialidase from influenza virus A/Tern/Australia/G70C/75 was purified as described previously[18] and crystallized by standard protocols[19] in 1.9 M phosphate (pH 5.9). The sialidase−5-(acetylamino)-4-amino-6-(phenethylpropylcarbamoyl)-5,6-dihydro-4*H*-pyran-2-carboxylic acid complex was prepared by soaking crystals in buffered solution containing 5 mM concentration of inhibitor over 24 h. X-ray diffraction data were collected on a Rigaku R-AXIS II imaging plate X-ray detector mounted on a MAC Science SRAM18XH1 rotating anode X-ray generator, operating at 47 kV and 60 mA with focusing mirrors. A total of 119 194 observations were measured to 2.0 Å and reduced to 23 918 unique reflections with a mean *R*-factor for symmetry related reflections of 0.075 and a merging *R*-factor of 0.096 over all the observations (mean $I/\sigma I = 6.6$). The space group is cubic, *I*432, with unit cell dimension $a = 182.8$ Å. The inhibitor was located by difference Fourier methods using phases from the native structure.[20] All the atoms of the inhibitor were identified, and the new orientation of Glu 276 was observed in the difference Fourier map. A model of the complex was built using the graphics program O[21] using the native structure with the active-site waters removed. The refinement was carried out using X-PLOR[22] with energy restraints[23] using data from 6.0 to 2.0 Å with a 2σ cutoff. Additional water molecules in the active site and elsewhere were then identified by difference Fourier methods during the course of the refinement. The final *R*-factor for the complex was 15.5% (6.0−2.0 Å) with rms deviations from ideal bonds and angles of 0.014 Å and 1.90°, respectively, and a mean *B*-value of 20.8 Å^2 for the refined non-hydrogen atoms. The coordinates of the complex have been deposited in the Brookhaven DataBank (code 1BJI).

Crystals of influenza B/Beijing/1/87 sialidase were grown from 7−10% PEG8K, 100 mM Tris/HCl at pH 7.5−8.0, in a modification of the published procedure.[24] They are grown by seeding, at room temperature, and reach their full size over 3 days. The crystals are trigonal bipyramids which are typically 0.1 mm × 0.1 mm × 0.2 mm in dimension. The complex between the sialidase and the inhibitor was formed by harvesting the crystal into 10% PEG8K and soaking it overnight in a 1 mM solution of **5d**. The crystal was then transferred into a solution containing 1 mM inhibitor in 10% PEG8K and 20% glycerol for 40 min prior to cryocooling. Reflection data were collected using 0.89-Å wavelength radiation at a temperature of 100 K on station 9.6 at the Synchrotron Radiation Source, Daresbury. A 30-cm MAR image plate was used to record 2° rotation images which were processed using MOSFLM.[25] For the complex with **1** a total of 140 043 observations were measured and reduced to 50 283 unique reflections after merging. The final dataset was 98% complete (34−2.2 Å) with $R_{merge} = 0.128$ and mean multiplicity of 2.7. The space group is $P3_121$ with unit cell dimensions $a = b = 88.2$ Å, $c = 221.1$ Å. For compound **5d** a total of 208 669 observations were measured and reduced to 77 084 unique reflections after merging. The final dataset was 97.4% complete (34−1.9 Å) with $R_{merge} = 0.092$ and mean multiplicity of 2.7. Unit cell parameters are $a = b = 88.3$ Å, $c = 221.1$ Å.

The binding mode of inhibitors **1** and **5d** to the active site of sialidase B was determined from an initial $F_o - F_c$ electron density map, using phases based on the complex with sialic acid (PDB entry 1nsc) after removing the ligand and water molecules from the active sites. Model building of the compounds was performed in QUANTA,[26] and refinement of the complexes (positional and independent *B*-factor) was carried out in X-PLOR.[22] The final *R*-factor for **1** was 19.8% for all data to 2.2 Å, while for **5d** it was 20.1% for all data to 1.9 Å. Overall deviations from ideal bond and angle parameters are 0.009 Å and 2.5° for **1** and 0.013 Å and 2.7° for **5d**, respectively. Coordinates for complexes with **1** and **5d** have been deposited in the Brookhaven DataBank (codes 1a4g and 1a4q).

Molecular Modeling. For each protein−ligand complex, 15 low-energy structures were generated using a molecular dynamics (MD) protocol in which the trajectories for the atomic motions were periodically randomized. Prior to the MD calculations the ligands were manually docked into an energy-minimized crystal structure, with a position and conformation similar to that of zanamivir, **1**. The phenethyl part of the carboxamide substituent was docked into the trans-pocket, and the cis-group was positioned either directly above residue Glu 276 (for the shorter groups) or between residues Glu 276 and Arg 292 (for the longer groups). The conformation of Glu 276 in each case corresponded to its conformation in the uncomplexed enzyme, with the acid group pointing up into the binding site (which is also its conformation in the complex with substrate and in the complex with zanamivir, **1**). Influenza A (Tern/N9) and influenza B (B/Beijing) sialidases were included in the study. The molecular dynamics and energy minimization calculations were done using the CVFF force field within the modeling package Discover[27] (Molecular Simulations Inc., San Diego, CA). Each calculation involved a total of 70 ps of constrained dynamics at 350 K and 33 000 iterations of energy minimization, requiring approximately 12 h of Silicon Graphics Power Challenge (CPU R8000) server time. The conformational flexibility of the ligand, a large number of protein residues, and a shell of solvent molecules around the active site were all explicitly included in the calculations. A distance-dependent dielectric was applied, and three different approaches to modeling the electrostatics were investigated: (a) using a nonbond cutoff distance of 8.5 Å, (b) applying a longer cutoff of 12.5 Å, and (c) defining the carboxylic acid and amine functional groups as a single, neutral entity, rather than two independent, unit-charge groups as in approaches a and b.[27] The results obtained from the different methods were qualitatively similar, although

some minor discrepancies were observed. Only the results from model a are discussed below.

The intermolecular binding energy was calculated for each complex by summing all pairwise atomic nonbonded interactions between protein and ligand. In CVFF, these interactions have a van der Waals component (12−6 potential) and a Coulombic contribution. To take into account the changes associated with protein intramolecular energies, active-site amino acid residue energies were also examined (a total of 19 residues were included in the analysis). For the set of residues, the energy terms for bond stretching and bending, torsion forces, and nonbonded van der Waals and Coulombic forces were all investigated, both independently of each other and summed together. For the set of 15 energy-minimized structures with each inhibitor, both the minimum energy values and the averaged energy values were analyzed.

Acknowledgment. We thank A. van Donkelaar and J. McKimm-Breshkin for their contributions to the protein crystallography and K. Cobley, A. Whittington, and H. Weston for their assistance with the chemistry.

References

(1) von Itzstein, M.; Wu, W.-Y.; Kok, G. B.; Pegg, M. S.; Dyason, J. C.; Jin, B.; Van Phan, T.; Smythe, M. L.; White, H. F.; Oliver, S. W.; Colman, P. M.; Varghese, J. N.; Ryan, D. M.; Woods, J. M.; Bethell, R. C.; Hotham, V. J.; Cameron, J. M.; Penn, C. R. Rational Design of Potent Sialidase-Based Inhibitors of Influenza Virus Replication. *Nature* **1993**, *363*, 418−423.

(2) Hayden, F. G.; Lobo, M.; Esinhart, J.; Hussey, E. Efficacy of 4-Guanidino Neu5Ac2en in Experimental Human Influenza A Virus Infection. 34th Interscience Conference on Antimicrobial Agents and Chemotherapy, Orlando, FL, Oct. 4−7, 1994; American Society for Microbiology: Washington, DC, 1994; p 190.

(3) Smith, P. W.; Sollis, S. L.; Howes, P. D.; Cherry, P. C.; Cobley, K. N.; Taylor, H.; Whittington, A. R.; Bethell, R. C.; Taylor, N. R.; Varghese, J. N.; Colman, P. M.; Singh, O.; Skarzynski, T.; Cleasby, A.; Wonacott, A. Novel Inhibitors of Sialidases Related to GG167. Structure−Activity, Crystallography, and Molecular Dynamics Studies with 4-H-Pyran-2-carboxylic Acid 6-Carboxamides. *Bioorg. Med. Chem. Lett.* **1996**, *6*, 2931−2936.

(4) Colman, P. M.; Varghese, J. N.; Laver, W. G. Structure of the Catalytic and Antigenic Sites in Influenza Virus Neuraminidase. *Nature* **1983**, *303*, 41−44.

(5) Varghese, J. N.; Laver, W. G.; Colman, P. M. Structure of the Influenza Virus Glycoprotein Antigen Neuraminidase at 2.9 Å Resolution. *Nature* **1983**, *303*, 35−40.

(6) Varghese, J. N.; Colman, P. M. The Three-Dimensional Structure of the Neuraminidase of Influenza Virus A/Tokyo/3/67 at 2.2 Å Resolution. *J. Mol. Biol.* **1991**, *221*, 473−486.

(7) Tulip, W. R.; Varghese, J. N.; Baker, A. T.; Van Donkelaar, A.; Laver, W. G.; Colman, P. M. The Refined Structures of N9 Subtype Influenza Neuraminidase and Escape Mutants. *J. Mol. Biol.* **1991**, *221*, 487−497.

(8) Burmeister, W. P.; Ruigrok, R. W. H.; Cusack, S. The 2.2 Å Resolution Crystal Structure of Influenza B Neuraminidase and its Complex with Sialic Acid. *EMBO J.* **1992**, *11*, 49−56.

(9) Janakiraman, M. N.; White, C. L.; Laver, W. G.; Air, G. M.; Luo, M. Structure of Influenza Virus Neuraminidase B/Lee/40 Complexed with Sialic Acid and a Dehydro Analogue at 1.8 Å Resolution: Implications for the Catalytic Mechanism. *Biochemistry* **1994**, *33*, 8172−8179.

(10) Varghese, J. N.; Epa, V. C.; Colman, P. M. Three-Dimensional Structure of the Complex of 4-guanidino-Neu5Ac2en and Influenza Virus Neuraminidase. *Protein Sci.* **1995**, *4*, 1081−1087.

(11) Varghese, J. N.; McKimm-Breschkin, J. L.; Caldwell, J. B.; Kortt, A. A.; Colman, P. M. The Structure of the Complex Between Influenza Virus Neuraminidase and Sialic Acid, the Viral Receptor. *Proteins* **1992**, *14*, 327−332.

(12) Burmeister, W. P.; Henrissat, B.; Bosso, C.; Cusack, S.; Ruigrok, R. W. H. Influenza B Virus Neuraminidase Can Synthesize Its Own Inhibitor. *Structure* **1993**, *1*, 19−26.

(13) Montgomery, J. A.; Niwas, S.; Rose, J. D.; Secrist, J. A., III; Babu, Y. S.; Bugg, C. E.; Erion, M. D.; Guida, W. C.; Ealick, S. E. Structure-Based Design of Inhibitors of Purine Nucleoside Phosphorylase. 1. 9-(Arylmethyl) Derivatves of 9-Deazaguanine. *J. Med. Chem.* **1993**, *36*, 55−69.

(14) Taylor, N. R.; von Itzstein, M. Molecular Modeling Studies on Ligand Binding to Sialidase from Influenza Virus and the Mechanism of Catalysis. *J. Med. Chem.* **1994**, *37*, 616−624.

(15) Taylor, N. R.; von Itzstein, M. A Structural and Energetic Analysis of the Binding of a Series of *N*-Acetylneuramminic Acid Based Inhibitors to Influenza Virus Sialidase. *J. Comput.-Aided Mol. Des.* **1996**, *10*, 233−246.

(16) Williams, D. H.; Cox, J. P. L.; Doig, A. J.; Garner, M.; Gerhard, U.; Kaye, P. T.; Lal, A. R.; Nicholls, I. A.; Salter, C. J.; Mitchell, R. C. Toward the Semiquantitative Estimation of Binding Constants. Guides for Peptide-Peptide Binding in Aqueous Solution. *J. Am. Chem. Soc.* **1991**, *113*, 7020−7030.

(17) Schulz, G. E.; Schirmer, R. H. *Principles of Protein Structure*; Springer-Verlag: New York, 1990; pp 36−41.

(18) McKimm-Breschkin, J. L.; Caldwell, J. B.; Guthrie, R. E.; Kortt, A. A. A New Method for the Purification of Influenza A Virus. *J. Virol. Methods* **1991**, *32*, 121−124.

(19) Laver, W. G.; Colman, P. M.; Webster, R. G.; Hinshaw, V. S.; Air, G. M. Influenza Virus Neuraminidase with Haemagglutinin Activity. *Virology* **1984**, *137*, 314−323.

(20) Tulip, W. G.; Varghese, J. N.; Baker, A. T.; van Donkelaar, A.; Laver, W. G.; Webster, R. G.; Colman, P. M. Refined Atomic Structures of N9 Subtype Influenza Virus Neuraminidase and Escape Mutants. *J. Mol. Biol.* **1991,** *221*, 487−497.

(21) Jones, T. A.; Zou, J. Y.; Kjeldgaard, M. Improved Methods for Building Protein Models in Electron Density Maps and Location of Errors in these Models. *Acta Crystallogr. A* **1991**, *47*, 110−119.

(22) Brunger, A. T. *X-PLOR, Version 3.3. A System for X-ray Crystallography and NMR*; Yale University Press: New Haven, CT, 1992.

(23) Engh, R. A.; Huber, R. Accurate Bond and Angle Parameters for X-ray Protein-Structure Refinement. *Acta Crystallogr. A* **1991**, *47*, 392−400.

(24) Burmeister, W. P.; Daniels, R. S.; Dayan, S.; Gagnon, J.; Cusack, S.; Ruigrok, R. W. H. Sequence and Crystallisation of Influenza Virus B/Beijing/1/87 Neuraminidase. *Virology* **1991**, *180*, 266−272.

(25) Leslie, A. G. W.; Brick, P.; Wonacott, A. J. MOSFLM. *Daresbury Lab. Inf. Quart. Protein Crystallogr.* **1986,** *18*, 33−39.

(26) *QUANTA96 X-ray Structure Analysis, User's Reference*; Molecular Simulations Inc.: San Diego, CA, 1996.

(27) *Discover 2.9.7/95.0/3.0.0. Forcefield Simulations. User Guide, Part 1*; Molecular Simulations Inc.: San Diego, CA, 1995; pp 2-12−2-14.

JM9703754